RPA Calculations and Analysis of the Electronic States of Cyclopropane and of the Chiroptical Properties of Its Methyl Derivatives

Steve Bohan† and Thomas D. Bouman*

Contribution from the Department of Chemistry, Southern Illinois University, Edwardsville, Illinois 62026. *Received December 2, 1985*

Abstract: Ab initio, extended basis set calculations in the random-phase approximation (RPA) are reported for the low-lying singlet electronic excitations of cyclopropane, *trans*-1,2-dimethylcyclopropane, and *trans*-1,2,2,3-tetramethylcyclopropane. For the chiral derivatives, the rotatory strengths are computed as well and analyzed into bond–bond coupling terms with the aid of localized orbitals. The computed chiroptical properties agree well with experiment, apart from an overall shift in the computed excitation energies. An apparent stereochemical anomaly regarding the chiral derivatives is explained by considering the nature of the low-lying excitations in each case.

I. Introduction

The electronic states of cyclopropane (**1**; see Figure 1), as the prototype three-membered ring system, and of its derivatives are of interest in a number of areas, including studies of the conjugative ability of the cyclopropyl group and mechanistic studies of carbene insertions to olefins.[1] The simplest chiral derivative of cyclopropane, *trans*-1,2-dimethylcyclopropane, in the enantiomer with a positive long-wavelength CD band, has been shown to have the absolute configuration (1*R*,2*R*)-**2**.[2] Subsequently, this well-established assignment was used to assign absolute configurations to several related compounds on the basis of the similarity of their CD spectra.[3]

Curiously, however, (1*R*,3*R*)-*trans*-1,2,2,3-tetramethylcyclopropane (**3**) has been shown to have the *same*-signed long-wavelength CD band as **2**, notwithstanding the fact that the *trans*-dimethyl moiety in **3** has the *opposite* absolute configuration to that in **2**.[4]

The purpose of this communication is to elucidate the UV and CD spectra of the methylcyclopropanes **2** and **3** through ab initio extended basis set calculations including electron correlation and through a detailed analysis of the computed rotatory strengths in terms of molecular structural features. We will model the low-lying excitations in the random-phase approximation (RPA), which yields the correct linear response of the Hartree–Fock ground state of a molecule to an external perturbation such as electromagnetic radiation.[6-8] We include calculations on cyclopropane itself to establish a benchmark for the chiral derivatives and to allow comparisons with other work.

II. Methods, Geometries, and Basis Sets

The methods used in these calculations have been described elsewhere[7,8] and are reviewed briefly below. The experimental geometry[9] was used for cyclopropane, and geometries for DMC (**2**) and TMC (**3**) were obtained by molecular mechanics (MM2)[10] calculations under the constraint of C_2 symmetry. The ring carbons in all three molecules are placed in the x–y plane, and the x axis is chosen as the common C_2 rotation axis in all cases. After some experimentation with basis sets, we chose the standard 5/31G set of Hehre et al.,[11] augmented by a single set of diffuse s-, p-, and d-type ($l = 2$) Gaussian functions ($\alpha_s = 0.011$, $\alpha_p = 0.015$, and $\alpha_d = 0.020$) on the center of the ring, a set of five Gaussian d functions ($\alpha_d = 0.97$) on each ring carbon, and an additional s-type Gaussian ($\alpha_s = 0.025$) on each ring hydrogen. On the methyl hydrogens, only a single (5s)/[1s] contracted Gaussian function was used. Thus both polarization effects and low-lying Rydberg states should be at least partly accounted for. The SCF ground-state wave functions were generated by the GAUSSIAN 80 program system,[12] and the electronic excitation spectrum was calculated in the random-phase approximation (RPA), using PROGRAM RPAC.[7] The RPA is particularly well suited to calculating electronic transition moments in which first-order correlation effects have been incorporated, and similarly correlated excitation energies are obtained as eigenvalues of a non-Hermitian eigenproblem. In the notation we will employ in this paper, the electric dipole length transition moment between the ground state $|0\rangle$ and excited state $|q\rangle$ is given by eq 1 while the velocity form and the magnetic dipole transition

$$\langle 0|\mathbf{r}|q\rangle = 2^{1/2} \sum_{am} \langle \alpha|\mathbf{r}|m\rangle S_{am,q} \tag{1}$$

moment are given, respectively, by eq 2 and 3. The coefficients $S_{am,q}$ and $T_{am,q}$ and the excitation energies ω_{0q} are obtained by solving the coupled

$$\langle 0|\hat{\nabla}|q\rangle = 2^{1/2} \sum_{am} \langle \alpha|\hat{\nabla}|m\rangle T_{am,q} \tag{2}$$

$$\langle 0|\mathbf{r} \times \hat{\nabla}|q\rangle = 2^{1/2} \sum_{am} \langle \alpha|\mathbf{r} \times \hat{\nabla}|m\rangle T_{am,q} \tag{3}$$

equations (4) where $A_{am,\beta n} = \langle \alpha \rightarrow m|\hat{H} - E_{HF}|\beta \rightarrow n\rangle$ and $B_{am,\beta n} = \langle HF|\hat{H}|\alpha \rightarrow m, \beta \rightarrow n\rangle$. Finally, α and β represent orbitals occupied in

$$(\mathbf{A} + \mathbf{B})\mathbf{S}_q = \omega_{0q}\mathbf{T}_q \tag{4a}$$

$$(\mathbf{A} - \mathbf{B})\mathbf{T}_q = \omega_{0q}\mathbf{S}_q \tag{4b}$$

the Hartree–Fock (HF) ground state, and m and n represent virtual MOs. The coefficients $S_{am,q}$ and $T_{am,q}$ in (4) obey the orthonormality condition in eq 5. Thus, an individual configuration αm contributes an

$$\sum_{am} S_{am,q} T_{am,p} = \delta_{qp} \tag{5}$$

amount $S_{am,q}T_{am,q}$ to the normalization of the overall excitation. In the RPA, *differences* in expectation values are obtained directly, as in eq 6, for a one-electron operator $\hat{A}$. The excitations and intensities were an-

† Present address: Department of Chemistry, University of California, Berkeley, CA 94720.

(1) For leading references, see: (a) Clark, T.; Spitznagel, G. W.; Klose, R.; Schleyer, P. v. R. *J. Am. Chem. Soc.* **1984**, *106*, 4412–4419. (b) Greenberg, A.; Liebman, J. F. *Strained Organic Molecules*; Academic: New York, 1978.
(2) Doering, W. von E.; Kirmse, W. *Tetrahedron* **1960**, *11*, 272–275.
(3) Moore, W. R.; Anderson, H. W.; Clark, S. D.; Ozretich, T. M. *J. Am. Chem. Soc.* **1971**, *93*, 4932–4934.
(4) Crombie, L.; Findlay, D. A. R.; King, R. W.; Shirley, I. M.; Whiting, D. A.; Scopes, P. M.; Tracey, B. M.; *J. Chem. Soc., Chem. Commun.* **1976**, 474–475.
(5) Mason, S. F., quoted in ref 4.
(6) For a recent review, see: Oddershede, J.; Jørgensen, P.; Yeager, D. L. *Comput. Phys. Rep.* **1984**, *2*, 33–92.
(7) Bouman, T. D.; Hansen, Aa. E.; Voigt, B.; Rettrup, S. *Int. J. Quantum Chem.* **1983**, *23*, 595–611.
(8) Hansen, Aa. E.; Bouman, T. D. *Adv. Chem. Phys.* **1980**, *44*, 545–644.
(9) Fritchie, C. J., Jr. *Acta Crystallogr.* **1966**, *20*, 34.
(10) Allinger, N. L. *J. Am. Chem. Soc.* **1977**, *99*, 8127.
(11) Hehre, W. J.; Stewart, R. H.; Pople, J. A. *J. Chem. Phys.* **1969**, *51*, 2557.
(12) Van Kampen, P. N.; de Leeuw, F. A. A. M.; Smits, G. F.; Altona, C. *QCPE* **1982**, *437*. Pople, J. A., et al. *QCPE* **1981**, *406*.

0002-7863/86/1508-3261$01.50/0

Table I. Computed Excitations for Cyclopropane

	assignment	ΔE^a	f^{v} (±)[b]	leading configs	% of norm[c]	$\Delta\langle x^2\rangle^d$	$\Delta\langle z^2\rangle$	notes	expt[e]
1	1E′	8.33	0.001 (0.000)	3e′ → 4a₁′	64	13.6	22.6	3e′ → 3s	band I: 7.4–8.2 eV, f = 0.12
2	1E″	8.69		3e′ → 2a₂″	49	9.8	31.5	3e′ → 3p$_z$	
				3e′ → 3a₂″	44				
3	1A₂′	8.84		3e′ → 4e′	56	23.5	12.9		
4	2A₁′	8.86		3e′ → 4e′	52	25.1	13.4	3e′ → 3p$_{x,y}$	
5	2E′	8.95	0.192 (0.000)	3e′ → 4e′	56	24.1	16.3		
6	3E′	9.72	0.000 (0.000)	3e′ → 5a₁′	86	30.5	19.6		band II: 8.3–8.9 eV, f = 0.04
7	1A₂″	9.94	0.005 (0.002)	3e′ → 2e″	92	24.0	40.1		
8	1A₁	9.95		3e′ → 2e″	82	21.6	35.8		
9	2E″	9.96		3e′ → 2e″	84	22.8	39.7	3e′ → 3d	
10	4E′	9.98	0.002 (0.000)	3e′ → 5e′	96	33.9	12.5		
11	2A₂′	10.00		3e′ → 5e′	99	34.6	11.7		
12	3A₁′	10.08		3e′ → 5e′	84	41.4	15.7		
13	3E″	10.22		3e′ → 2a₂″	47	26.3	91.7		
				3e′ → 3a₂″	42				
14	3A₂′	10.33		3e′ → 6e′	52	59.7	29.3		
15	5E′	10.35	0.068 (0.031)	3e′ → 6e′	45	52.7	34.7		
16	4A₁′	10.45		3e′ → 6e′	61	54.1	26.0		
17	6E′	10.63	0.062 (0.012)	3e′ → 6a₁′	55	27.8	46.6		band III: 9.2–10.5 eV, f = 0.7
18	4E″	10.80		1e″ → 4a₁′	45	14.5	18.0		
				1e″ → 6a₁′	19				
19	2A₁″	11.16		3e′ → 3e″	79	28.7	37.9		
20	2A₂″	11.21	0.190 (0.007)	3e′ → 3e″	49	25.0	24.7		
				1e″ → 4e′	19				
				1e″ → 6e′	19				
21	5E″	11.25		3e′ → 3e″	84	26.8	35.7		
22	7E′	11.41	0.316 (0.011)	1e″ → 2a₂″	44	10.0	30.0	$\pi \rightarrow \pi^*$-like	
				1e′ → 3a₂″	35				
				3e′ → 1a₂′	5				
23	3A₂″	11.45	0.041 (0.004)	1e″ → 4e′	29	25.0	20.7		
				3e′ → 3e″	41				
				1e″ → 6e′	22				
24	3A₁″	11.67		1e″ → 4e′	53	27.3	12.1		
25	6E″	11.87		1e″ → 4e′	48	22.2	23.4		
				1e″ → 6e′	19				
26	8E′	12.40	0.495 (0.016)	3e′ → 1a₂′	71	5.9	14.5	valence	

[a] Energies in eV. [b] (±) is half the difference between the length and velocity forms of f. [c] Equation 5. [d] From eq 6. $\Delta\langle y^2\rangle = \Delta\langle x^2\rangle$ by symmetry, and $\Delta\langle r^2\rangle = \Delta\langle x^2\rangle + \Delta\langle y^2\rangle + \Delta\langle z^2\rangle$. [e] Reference 15a.

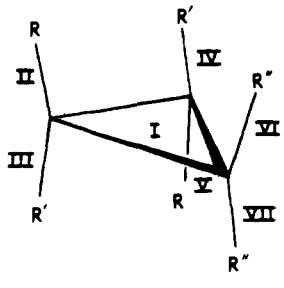

(CYP) 1: R=R′=R″=H

(DMC) 2: R′=R″=H, R=CH$_3$

(TMC) 3: R′=R″=CH$_3$, R=H

Figure 1. Absolute configurations and bond numbering scheme for compounds **1–3**. Bond set I includes the three ring bonds, while bond sets II–VII include the bonds in their respective substituents as well as the bond to the ring carbon.

alyzed into coupling terms among the bonds of the molecules using the localized orbital analysis scheme presented earlier;[13] a brief summary is included in section IV.

$$\Delta\langle A\rangle \equiv \langle q|\hat{A}|q\rangle - \langle 0|\hat{A}|0\rangle = \tfrac{1}{2}\sum_{\alpha m}\sum_{\beta n}\{S_{\alpha m,q}S_{\beta n,q} + T_{\alpha m,q}T_{\beta n,q}\}\{\langle m|\hat{A}|n\rangle\delta_{\alpha\beta} - \langle\alpha|\hat{A}|\beta\rangle\delta_{mn}\} \quad (6)$$

(13) Hansen, Aa. E.; Bouman, T. D. *J. Am. Chem. Soc.* **1985**, *107*, 4828–4839.

III. Results

An overview of the results is presented in Figure 2; the individual molecules will be discussed below. From the figure, one sees first of all that the lowest (degenerate) pair of excitations in **1** is well separated from the next group near 8.8 eV, which in turn is separated by a gap of nearly 0.7 eV from a dense manifold of excitations extending over the next 1.1-eV range. In **2**, one sees the expected red shift of the spectrum due to methylation, and the lowest eight states are still well separated from the dense set of excitations beginning around 9.1 eV. In **3**, an additional red shift occurs, and the states that split in **2** are more nearly degenerate in **3**. Otherwise, the pattern is similar.

Cyclopropane. The basis set described in the previous section contains 69 orbitals and yields an SCF energy of −117.031 969 hartrees. All calculations were carried out using the D_{3h} ground-state geometry; the configurations and excited states are labeled with D_{3h} symmetries. The orbital basis yields 513 particle-hole excitations, excluding the excitations out of the carbon 1s orbitals, and all of these were used directly in the RPA calculations, without symmetry blocking.

The computed singlet excitations up through the first "valence" excitation are presented in Table I. Apart from consistently overestimated excitation energies relative to both experiment and other calculations, which will be discussed later, the following points may be noted. All excitations below 10.7 eV are computed to arise out of the 3e′ orbital pair; the large $\Delta\langle r^2\rangle$ values show that these are Rydberg-type excitations. The 4a₁′, 2a₂″, and 4e′ orbitals have the character of Rydberg 3s, 3p$_z$, and 3p$_{x,y}$ orbitals, respectively, while the 5a₁′, 2e″, and 5e′ MOs resemble Rydberg 3d$_0$, 3d$_{\pm1}$, and 3d$_{\pm2}$ orbitals. In many of the excitations of cyclopropane and its methyl derivatives, we find that the transition can be represented (after the fact) to a good approximation as a simple promotion of an electron out of a particular occupied

Table II. Computed Singlet Excitations for DMC and TMC

	assignment	ΔE^a	nature	%[b]	f^V (±)[c]	$R^d(\Delta)^e$
			DMC			
1	1A	7.82	$\phi_{20} \rightarrow 3s$	93	0.008 (0.001)	17.4 (3.9)
2	1B	7.95	$\phi_{20} \rightarrow 3p_\perp$	70	0.002 (0.000)	12.8 (3.1)
3	2B	8.14	$\phi_{19} \rightarrow 3s$	63	0.002 (0.000)	−6.5 (0.2)
4	2A	8.29	$\phi_{20} \rightarrow 3p_x$	85	0.002 (0.000)	−0.3 (0.0)
5	3A	8.33	$\phi_{19} \rightarrow 3p_\perp$	80	0.027 (0.000)	−15.8 (0.3)
6	3B	8.37	$\phi_{20} \rightarrow 3p_\parallel$	87	0.033 (0.004)	−8.1 (2.6)
7	4B	8.59	$\phi_{19} \rightarrow 3p_x$	92	0.008 (0.000)	−4.0 (2.3)
8	4A	8.69	$\phi_{19} \rightarrow 3p_\parallel$	92	0.000 (0.000)	2.6 (1.1)
9	5A	9.08	$\phi_{20} \rightarrow 3d$	94	0.013 (0.001)	−2.5 (0.2)
			TMC			
1	1B	7.57	$\phi_{28} \rightarrow 3s$	87	0.009 (0.002)	11.5 (2.1)
2	1A	7.63	$\phi_{27} \rightarrow 3s$	77	0.000 (0.001)	6.8 (7.2)[f]
3	2A	7.91	$\phi_{28} \rightarrow 3p_\perp$	77	0.001 (0.000)	3.3 (0.3)
4	2B	7.92	$\phi_{27} \rightarrow 3p_\perp$	80	0.009 (0.001)	−16.0 (2.5)
5	3A	8.04	$\phi_{28} \rightarrow 3p_\parallel$	95	0.024 (0.004)	−3.2 (0.5)
6	3B	8.04	$\phi_{28} \rightarrow 3p_x$	85	0.011 (0.004)	12.8 (3.9)
7	4B	8.11	$\phi_{27} \rightarrow 3p_\parallel$	93	0.009 (0.002)	−5.2 (0.8)
8	4A	8.17	$\phi_{27} \rightarrow 3p_x$	95	0.020 (0.007)	−0.8 (0.3)
9	5A	8.61	$\phi_{28} \rightarrow 3d$	95	0.021 (0.002)	10.4 (0.9)

[a] Energies in eV. [b] Percent of normalization, eq 5. [c] (±) defined as in Table I. [d] Units of R are cgs × 10^{40}. [e] $(\Delta) = R^V - R^r$. [f] Signs of R^V and R^r are opposite.

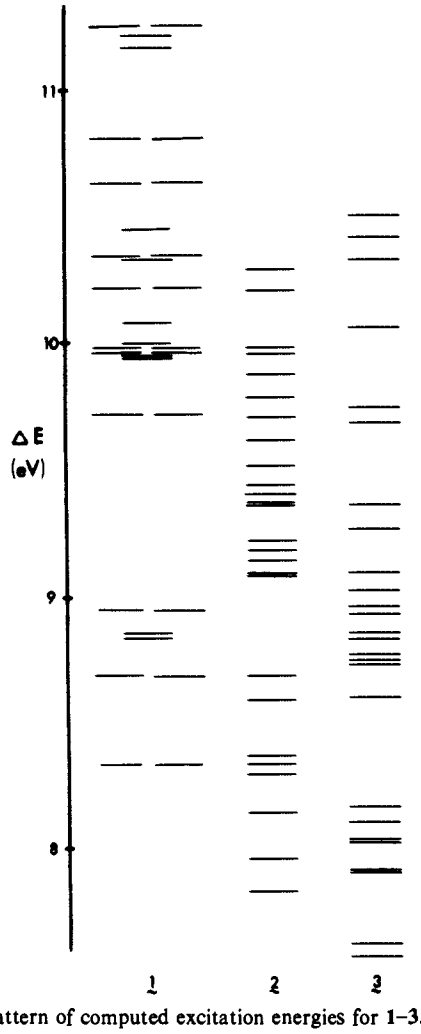

Figure 2. Pattern of computed excitation energies for 1–3.

orbital into a linear combination of canonical virtual orbitals. We term this combination an effective virtual orbital (EVO).[14] The effective $3p_z$ upper orbital is represented by an EVO consisting of a roughly equal mixture of the $2a_2''$ and $3a_2''$ MOs.

The lowest singlet excitation is computed to be the $3e' \rightarrow 3s$ transition at 8.33 eV. The 1E'', $1A_2'$, $2A_1'$, and 2E' excitations between 8.69 and 8.95 eV arise from the $3e' \rightarrow 3p$ manifold. This 8.33–8.95-eV band has a total oscillator strength of 0.19 and is plausibly correlated with the observed long-wavelength band at 7.4–8.2 eV with $f = 0.12$.[15a] Moreover, the splitting pattern of the 3p orbitals agrees with that discussed by Robin.[15b]

The second observed band in cyclopropane, from 8.3 to 8.9 eV with $f = 0.04$,[15a] correlates with the present computed excitations 6–15, from 9.72 to 10.35 eV, with a total oscillator strength of 0.08. Most of the intensity is carried by the 5E' ($3e' \rightarrow 6e' + 4e'$) excitation. In the region from 10.45 to 11.87 eV, we compute 10 excitations, carrying a total intensity of 0.68. This region may be associated with the 9.2–10.5-eV "valence" band with $f = 0.7$,[15a] despite the apparent Rydberg character of the excitations. The $\Delta\langle r^2\rangle$ values show that the 7E' excitation is considerably more compact than the others, indicating a mixture of Rydberg and valence character. Indeed, about 5% of the normalization of this excitation is due to the valencelike $3e' \rightarrow 1a_2'$ configuration that dominates the "true" valence excitation 8E' at 12.40 eV. The high intensity of 7E' can be ascribed to the $1e'' \rightarrow a_2''$ configurations: 1e'' has the nodal properties of an ethylenic π^* orbital, while the a_2'' orbitals transform like π. Thus, the $1e'' \rightarrow a_2''$ excitation should be strongly allowed, like an olefinic $\pi \rightarrow \pi^*$ transition.[16]

The overall agreement between the present results and the experimental spectrum is thus seen to be reasonable. The most extensive prior theoretical calculation on cyclopropane is that of Goldstein, Vijaya, and Segal (GVS),[17] who employed a CI scheme that treats single and double excitations out of a multiconfiguration reference set. Our results agree with theirs in the overall ordering of the excitations, although our larger atomic basis set leads to a higher density of states in the ca. 4-eV region of interest than was obtained by GVS. At the low-energy end, we compute a low-lying 1E'' excitation, as part of the 3p Rydberg manifold, which is absent in the GVS results. At the high end, we are able to account for the intensity of the third band without explicit recourse to the valence 8E' ($3e' \rightarrow 1a_2'$) excitation, thus avoiding the question that troubled GVS of the 1-eV gap between this excitation and the rest. On the other hand, the present results

(14) In ref 13, we used the term IVO to refer to this effective orbital; the change to EVO is to avoid confusion with the Hunt–Goddard formalism [Hunt, W. J.; Goddard, W. A. *Chem. Phys. Lett.* **1969**, *3*, 414].

(15) Robin, M. B. *Higher Excited States of Polyatomic Molecules*; Academic: New York, (a) 1975; Vol. 1. (b) 1985; Vol. 3.

(16) For a different interpretation of the intensity of this band, see: Robin, M. B. *Chem. Phys. Lett.* **1985**, *119*, 33.

(17) Goldstein, E.; Vijaya, S.; Segal, G. A. *J. Am. Chem. Soc.* **1980**, *102*, 6198–6204.

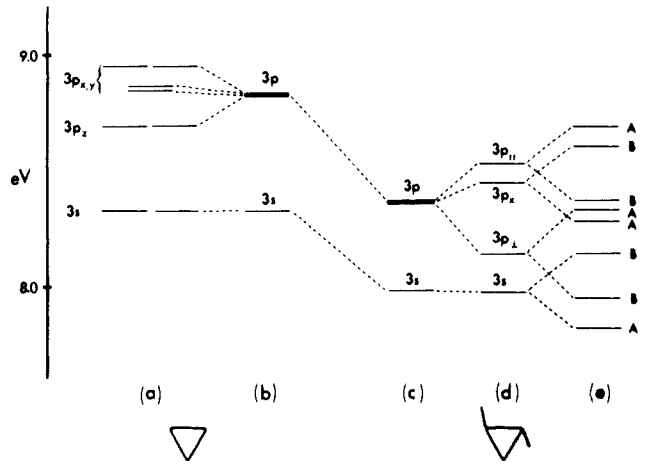

Figure 3. Relation of low-lying excitations in CYP and DMC. (a) Cyclopropane excitations in D_{3h} symmetry. (b) Centers of gravity of 3s and 3p Rydberg excitations in D_{3h}. (c) Red shift of centers of gravity upon methylation. (d) Splitting of 3p Rydberg EVOs in C_2 symmetry. (e) Further splitting due to lifting of degeneracy of highest occupied orbital pair in dimethyl cyclopropane.

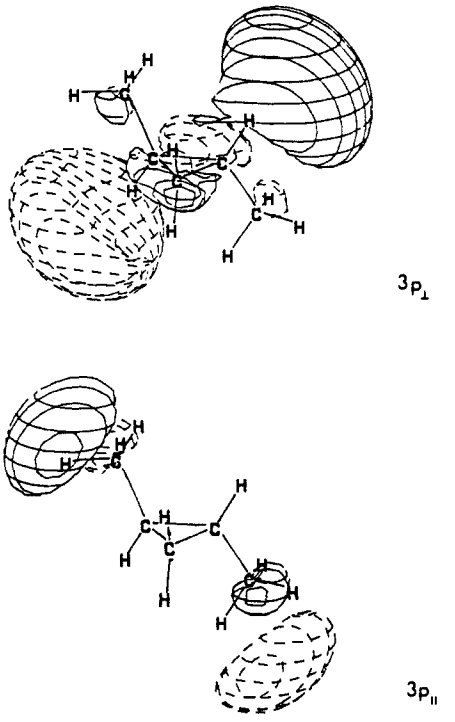

Figure 4. Requantization of 3p Rydberg EVOs in DMC. Jorgensen–Salem plots[21] of $3p_\perp$ and $3p_\parallel$ orbitals, evaluated at the 0.02-au contour level.

are consistently higher in energy than the GVS results. We believe that this energy shift reflects the importance of configurations that are triply excited relative to the Hartree–Fock ground state and of other higher-order terms that are absent in the RPA model. These terms appear to affect mainly the overall scale of the excitation energies and not the intensities.

Dimethylcyclopropane. The geometry for DMC was constrained to have C_2 symmetry. The MM2-optimized geometry with the 87-orbital basis described above yielded an SCF energy of −195.045 625 hartrees. The particle-hole basis for the RPA contained 503 configurations of A symmetry in the C_2 point group, and 502 of B symmetry, excluding excitations out of the five carbon "core" orbitals.

The results for the lowest few singlet excitations of dimethylcyclopropane are shown in Table II. All excitations below 10.5 eV arise out of the two highest occupied orbitals ϕ_{19} (9b) and ϕ_{20} (11a), which correlate closely with the 3e′ pair in cyclopropane. The lowering in symmetry from D_{3h} to C_2 causes extensive mixing among the erstwhile distinct symmetries of cyclopropane, and all excitations in DMC are both electric and magnetic dipole allowed. The form of the EVOs in this molecule shows that the perturbation brought about by the methyl groups is (not unreasonably) much greater on the low-lying Rydberg excitations than on the ground state.

The lowest excitations in DMC can be understood most easily with reference to (1) the perturbation of the methyl groups and (2) the descent in symmetry from D_{3h} to C_2 (Figure 3). In cyclopropane, the degenerate 3e′ → 3s excitations occur at 8.33 eV, while the center of gravity of the two related states in DMC (1A and 2B; see Table II) is at 7.98 eV, a red shift of 0.35 eV. The six states arising from 3e′ → 3p in cyclopropane have their center of gravity at 8.83 eV, while their counterparts in DMC have an average energy of 8.37 eV, giving a 0.46-eV red shift. The bulk of these red shifts can be ascribed to the raising of the orbital energies of the 3e′ pair by 0.76 eV upon (di-) methylation. Completing the descent in symmetry in a hypothetical second step causes the splitting of the erstwhile 3e′ orbital pair into ϕ_{19}, with *b* symmetry, and ϕ_{20}, with *a* symmetry, separated by 0.3 eV. This splitting, coupled with the split of the 3p manifold into $3p_\perp$, $3p_x$, and $3p_\parallel$ components (see Figure 4), accounts for the pattern displayed in Table II for the lowest eight singlet excitations in DMC.

The lowest two excitations, assigned as $\phi_{20} \rightarrow 3s$ and $\phi_{20} \rightarrow 3p_\perp$, form a band at 7.9 eV with a combined rotatory strength of $R^\nabla = +30$ (cgs × 10^{40}) and a total oscillator strength $f^\nabla = 0.01$. This band thus correlates well with the strong CD cotton effect and concomitant weak absorption observed at 190 nm by Gedanken and Schnepp.[18] (These authors obtained their measurements on the (1*S*,2*S*) enantiomer of DMC; all CD signs are therefore reversed in comparing their results with ours.)

The next six excitations, into Rydberg 3s and 3p orbitals and spanning the range 8.1–8.7 eV, carry a total $R^\nabla = -32$ and a total $f^\nabla = 0.07$. We assign the CD band at 177 nm, opposite in sign to the first, to this group of closely spaced excitations, with the main contribution to the CE coming near 8.3 eV and arising from the nearly degenerate pair of excitations $\phi_{19} \rightarrow 3p_\perp$ and $\phi_{20} \rightarrow 3p_\parallel$.

The third CD band in DMC, located at 160 nm and also negative in our enantiomer, corresponds with a monotonically increasing UV absorption. The observed separation of ca. 1.3 eV between this peak and the first band suggests a correlation with excitations computed to lie above 9 eV. We compute a very high density of states in this region, with 16 excitations falling between 9 and 10 eV. Several of these have quite large positive or negative rotatory strengths, although the net total R^∇ in this region is only +4, while the total intensity is $f^\nabla = 0.21$. The intensity adequately accounts for the increasing UV absorption, but how the various states might interfere to yield the observed CE sign is problematical. As we have found in a recent study of chiral monoolefins,[13] large redistributions of rotatory intensity can accompany relatively small changes in the energies of configurational makeup among closely spaced excitations. At this point, therefore, we will content ourselves with identifying the observed third band in DMC with the manifold of states calculated from 9 to 10 eV.

Tetramethylcyclopropane. For TMC, the basis set includes 105 atomic orbitals, and the MM2 geometry yielded an SCF energy of −273.052 672 hartrees. As with DMC, the particle-hole basis for the RPA was symmetry-adapted (C_2 point group), with 809 A configurations and 808 B configurations. The computed low-lying singlet excitations are given in Table II and Figure 1. At the long-wavelength end is a pair of closely spaced excitations around 7.6 eV, which we assign as $(\phi_{27}, \phi_{28}) \rightarrow 3s$. The lowest B state ($\phi_{28} \rightarrow 3s$) carries a computed rotatory intensity $R = +11.5$, while the signs of R^∇ and R^r differ for the lowest A state. The difficulty with the description of this state appears to be associated with the extremely feeble computed electric dipole transition moment, magnifying any errors in the projection of the

(18) Gedanken, A.; Schnepp, O. *Chem. Phys.* **1976**, *12*, 341–348.

Table III. Mechanistic Contributions to Rotatory Strength of Lowest Excitations in DMC and TMC

excitation	R^{∇}	intr.	μ–m	μ–μ
		DMC		
$\phi_{20} \rightarrow$ 3s	+17.4	−1.2	+7.0	+11.6
$\phi_{20} \rightarrow$ 3p	+12.8	+0.4	+3.3	+9.1
$\phi_{19} \rightarrow$ 3s	−6.5	+0.8	−1.7	−5.6
$\phi_{19} \rightarrow$ 3p	−15.8	+0.2	−3.5	−12.5
		TMC		
$\phi_{28} \rightarrow$ 3s	+11.5	−2.5	+6.9	+7.1
$\phi_{27} \rightarrow$ 3s	+6.8	+1.0	+1.2	+4.6
$\phi_{28} \rightarrow$ 3p	+3.3	+0.2	+1.2	+1.9
$\phi_{27} \rightarrow$ 3p	−16.0	+0.9	−4.5	−12.4

magnetic dipole transition moment on it. The sign of R^{∇} agrees with the experimental (+) CE in this band. Above this pair of excitations is a band from 7.9 to 8.2 eV consisting of the six 3p Rydberg excitations out of ϕ_{27} and ϕ_{28}. We predict a net negative CE for this set of states ($R^{\nabla}_{TOT} = -9$), with a net oscillator strength of 0.07. The B states in this manifold are responsible for most of the rotatory intensity, while the ordinary intensity is nearly evenly distributed among A and **B** states.

Only limited comparison with experiment is possible, since only $\Delta\epsilon_{max}$ and λ_{max} for the long-wavelength band in TMC have been reported.[4] We calculate the correct CE sign for this band, although the magnitude may be somewhat low.

The pattern of low-lying excitations in TMC resembles that in cyclopropane in some respects more than that in DMC. Table II shows that excitations into a given Rydberg orbital out of ϕ_{27} and ϕ_{28} are much more nearly degenerate in TMC than in DMC. Indeed, the orbital energies of the erstwhile 3e′ pair differ by only 0.14 eV in TMC, as compared with more than twice that in DMC. The addition of the *gem*-dimethyl group reduces the symmetry-lowering perturbation of the other two methyl groups so that the charge distribution of the relevant orbitals more closely approaches that of the original D_{3h} symmetry.

IV. Analysis of Intensities

The rotatory strength R^{∇}, given by eq 7, is well-known to be independent of the choice of origin of the coordinate system, but

$$R^{\nabla} = (2c\omega_{0q})^{-1}\langle 0|\hat{\nabla}|q\rangle\cdot\langle 0|\mathbf{r} \times \hat{\nabla}|q\rangle \qquad (7)$$

this is not necessarily true of the individual terms when R^{∇} is decomposed into contributions from, e.g., molecular fragments. We have recently shown[13] that the use of occupied localized MOs and the introduction of excitation-specific, effective "bond" transition moments of the form in eq 8, with a similar expression

$$\nabla_{\alpha,q} = 2^{1/2}\sum_{m}\langle\alpha|\hat{\nabla}|m\rangle T_{\alpha m,q} \qquad (8)$$

based on eq 3 for a bond magnetic dipole transition moment $\mathbf{l}_{\alpha,q}$, provides a decomposition of R^{∇} into terms that are individually origin invariant. In addition, these terms can be cast in the form of the three mechanisms suggested by Kirkwood, namely the "intrinsic", μ–m, and μ–μ terms.[19]

Thus, a general, origin-independent decomposition into bond–bond terms may be written as eq 9 where $R_{\alpha\beta}{}^{q} = (4c\omega_{0q})^{-1}\{\nabla_{\alpha,q}\cdot\mathbf{l}_{\beta,q} + \nabla_{\beta,q}\cdot\mathbf{l}_{\alpha,q}\}$. The diagonal terms $R_{\alpha\alpha}{}^{q}$ represent the intrinsic, or

$$R_{0q} = \sum_{\alpha}\sum_{\beta}R_{\alpha\beta}{}^{q} \qquad (9)$$

dissymmetric perturbation, mechanism, while the off-diagonal terms may be rewritten as eq 10 where $\mathbf{l}_{\alpha,q}{}'$ and $\mathbf{l}_{\beta,q}{}'$ are local

$$R_{\alpha\beta}{}^{q} + R_{\beta\alpha}{}^{q} = (4c\omega_{0q})^{-1}\{\nabla_{\alpha,q}\cdot\mathbf{l}_{\beta,q}{}' + \nabla_{\beta,q}\cdot\mathbf{l}_{\alpha,q}{}' + (\rho_{\alpha} - \rho_{\beta})\cdot\nabla_{\alpha,q} \times \nabla_{\beta,q}\} \qquad (10)$$

magnetic transition moments relative to the orbital centroid positions ρ_{α} and ρ_{β}, respectively. The first two terms on the right-hand side of eq 10 are μ–m coupling terms, while the last term is a μ–μ or "polarizability" coupling.[13]

In Table III, we show the contributions to R^{∇} from each of the three mechanisms for the lowest few excitations in DMC and TMC. Although all three mechanistic types contribute, the predominant couplings in each case are of the μ–μ type. Hence one would expect that semiempirical polarizability models of optical activity can account for the main features of the CD in these systems.

Having established the overall mechanism, we present a more detailed view of the $R_{\alpha\beta}{}^{q}$ terms in eq 7 in Tables IV–VII for the lowest excitations in DMC and TMC. For conciseness, we have grouped the bonds into seven sets, corresponding to the ring bonds and the six sets of substituent bonds C–R (R = H or CH_3) attached to the ring carbons (see Figure 1). Couplings between the ring bonds and the other bond sets are significant in all cases, with ring–CH_3 terms being consistently larger than ring–H terms. Trans CH_3–CH_3 couplings across the plane of the ring are also particularly large, but they are not always sign determining. Indeed, the distribution of the numbers shows that the detailed intensity mechanisms are quite different for all four excitations shown. Mason[5] has suggested that the apparent stereochemical anomaly between **2** and **3** can be rationalized as follows: if the *trans*-dimethyl moiety (II–I–V) in **2** is assumed to confer positive chirality on the ring, then the *gem*-dimethyl group in **3** provides two more *trans*-dimethyl moieties to the molecule (VI–I–III and IV–I–VII), each with positive chirality, thus more than balancing

Table IV. Analysis of R^{∇} into Groups of $R_{\alpha\beta}$ Terms (Equation 9) for the Lowest B Symmetry Excitation ($\phi_{28} \rightarrow$ 3s) in TMC. Groups of Bonds Are Defined in Figure 4

	I	II	III	IV	V	VI	VII
I	−7.2						
II	−0.6	0.0			$R_{TOT}{}^{\nabla}$ =	+11.5	
III	−1.7	0.6	0.3				
IV	−1.7	1.3	−2.7	0.3			
V	−0.6	−0.2	1.3	0.6	0.0		
VI	2.2	−1.6	8.5	2.1	−0.5	0.3	
VII	2.2	−0.5	2.1	8.5	−1.6	−0.4	0.3

Table V. Analysis of R^{∇}, as in Table IV, for the Lowest A Excitation ($\phi_{20} \rightarrow$ 3s) in DMC

	I	II	III	IV	V	VI	VII
I	−3.7						
II	−0.7	0.5			$R_{TOT}{}^{\nabla}$ =	+17.4	
III	0.0	−0.1	0.0				
IV	0.0	0.0	0.0	0.0			
V	−0.7	17.6	0.0	−0.1	0.5		
VI	0.6	1.6	0.0	0.0	−3.1	0.0	
VII	0.6	−3.1	0.0	0.0	1.6	−0.1	0.0

Table VI. Analysis of R^{∇}, as in Table IV, for the Lowest B Excitation ($\phi_{20} \rightarrow 3p_{\perp}$) in DMC

	I	II	III	IV	V	VI	VII
I	9.9						
II	3.9	−0.6			$R_{TOT}{}^{\nabla}$ =	+12.8	
III	1.2	1.0	0.0				
IV	1.2	1.0	0.0	0.0			
V	3.9	−1.5	1.0	1.0	−0.6		
VI	0.4	−2.4	0.1	0.1	−3.0	−0.1	
VII	0.4	−3.0	0.1	0.1	−2.4	0.8	−0.1

Table VII. Analysis of R^{∇}, as in Table IV, for the Second B Excitation ($\phi_{19} \rightarrow$ 3s) in DMC

	I	II	III	IV	V	VI	VII
I	−2.1						
II	2.9	−0.1			$R_{TOT}{}^{\nabla}$ =	−6.5	
III	−3.3	−2.2	0.0				
IV	−3.3	−3.5	0.8	0.0			
V	2.9	3.3	−3.5	−2.2	−0.1		
VI	0.6	0.5	−0.1	−0.4	1.5	0.0	
VII	0.6	1.5	−0.4	−0.1	0.5	0.3	0.0

(19) Kirkwood, J. G. *J. Chem. Phys.* **1937**, *5*, 479; **1939**, *7*, 139.

the negative chirality conferred by the coupling path III-I-IV. Mason's conjecture[5] is discernible in the 3s Rydberg excitations in both DMC and TMC: the II-V coupling in DMC is positive in both 1A and 2B, while the III-IV coupling in TMC (1B) is negative and the III-VI and IV-VII couplings are positive. This rule does not hold for the 3p Rydbergs, however, and in the 2B excitation of DMC, it does not determine the sign.

V. Concluding Remarks

The RPA in extended basis set calculations is capable of giving a good account of low-lying singlet electronic excitations, both in terms of energies and of oscillator and rotatory strengths. Even with basis sets of the size used here, however, one cannot claim that further basis optimization would not yield further improvement. Beyond that, the systematic overestimation of excitation energies, as compared with our previous work on planar monoolefins,[19] shows that higher-order effects are important for these strained-ring systems. As regards the stereochemical "puzzle" of DMC vs. TMC, the present calculations show that the long-wavelength CD bands are of different nature in the two molecules so that sign correlations are not to be anticipated. Because of the high density of states in cyclopropane and its derivatives, perhaps some caution is appropriate in assigning absolute configurations solely on the basis of correspondence of long-wavelength CD in these molecules.

Acknowledgment. Acknowledgment is made to the donors of the Petroleum Research Fund, administered by the American Chemical Society, for support of this research. This work was also supported in part by the National Science Foundation (CHE-82-18216). We thank the Data Processing and Computing Center of Southern Illinois University at Edwardsville for generous grants of computer time. Finally, we are grateful to Profs. Harry Morrison and William Jorgensen for providing us with a copy of the contour plot program, which we have adapted for PROGRAM RPAC.

(20) Bouman, T. D.; Hansen, Aa. E. *Chem. Phys. Lett.* **1985**, *117*, 461-467.
(21) (a) Jorgensen, W. L.; Salem, L. *The Organic Chemist's Book of Orbitals*; Academic: New York, 1973. (b) Morrison, H.; Jorgensen, W. L.; Bigot, B.; Severance, D.; Munoz-Sola, Y.; Strommen, R.; Pandey, B. *J. Chem. Educ.* **1985**, *62*, 298-301.

Oxygen Transfer from Iron Oxo Porphyrins to Ethylene. A Semiempirical MO/VB Approach

A. Sevin*† and M. Fontecave‡

Contribution from the Laboratoire de Chimie Organique Théorique, UA N° 506 CNRS, Bâtiment F, 75232 Paris, Cedex 05, France, and the Laboratoire de Chimie et Biochimie Pharmacologiques et Toxicologique, UA N° 400 CNRS, 75270 Paris, Cedex 06, France. *Received March 18, 1985*

Abstract: A semiempirical study of oxygen transfer from oxo porphyrins to ethylene is proposed, based on EHT calculations augmented by VB analysis of the resultant wave functions. It is shown that the Fe^{IV}–O chromophore bears a substantial radical character (Fe–O^0) and thus reacts like an RO^0 species. MO and state correlation diagrams are used in order to underline the major electronic events found along the various pathways. An interplay between adiabatic surfaces of even d^n configurations allows for the obtention of resultant diabatic surfaces corresponding to one-electron-transfer mechanisms. It is shown that the observed stereoselectivity results from the competition between potential energy barriers and rotation around the C–C bond in the intermediate radical. A qualitative VB picture of the reactivity is proposed which emphasizes the role of spin polarization.

Cytochrome P-450 monooxygenases catalyze the reductive activation of dioxygen by NADPH[1] and the insertion of one oxygen atom into various organic bonds such as in alkanes or alkenes according to the scheme below. The fact that exogenous

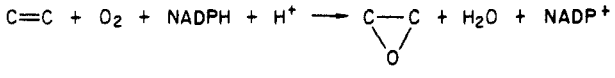

oxygen donors such as alkyl hydroperoxides[2] and iodosylbenzene[3] are effective oxygen atom sources for the hemoprotein in the absence of O_2 and a reducing agent has supported the view that the active transient species is an electrophilic oxoiron complex.[1] Two types of complexes have been considered: an iron(V) oxo complex **1** or an iron(IV) oxo porphyrin cation radical **2**.[1] In

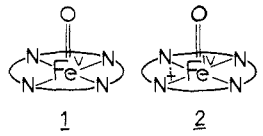

favor of structure **2** is the recent report that this radical is formed at low temperature upon the heme model reaction of an iron(III) porphyrin with iodosylbenzene or peroxybenzoic acid.[4] This species is able to efficiently epoxidize alkenes and has therefore been postulated as the active oxygen complex in the model oxidation of hydrocarbons catalyzed by synthetic iron porphyrins.[5] Several other ferryl complexes have been reported: (i) On the grounds of spectroscopic data, **2** has been shown to be a key intermediate in the mechanism of action of peroxidases (compound I of horseradish peroxidase (HRP) and catalase.[6,7] (ii) A por-

† Laboratoire de Chimie Organique Théorique.
‡ Laboratoire de Chimie et Biochimie Pharmacologiques et Toxicologique.

(1) Ulrich, V. *Top. Curr. Chem.* **1979**, *83*, 68.
(2) Nordblom, G. D.; White, R. E.; Coon, M. J. *Arch. Bichem. Biophys.* **1976**, *175*, 524.
(3) Ulrich, V.; Ruf, H. H.; Wende, P. *Croat. Chem. Acta* **1977**, *49*, 213.
(4) Groves, J. T.; Haushalter, R. C.; Nakamura, N.; Nemo, T. E.; Evans, B. J. *J. Am. Chem. Soc.* **1981**, *103*, 2884.
(5) (a) Groves, J. T.; Nemo, T. E.; Myers, R. S. *J. Am. Chem. Soc.* **1979**, *101*, 1032. (b) Groves, J. T.; Kruper, W. J.; Nemo, T. E.; Myers, R. S. *J. Mol. Catal.* **1980**, *7*, 169. (c) Chang, C. K.; Kuo, M. S. *J. Am. Chem. Soc.* **1979**, *101*, 3413. (d) Change, C. K.; Ebina, F. J. *J. Chem. Soc., Chem. Commun.* **1981**, 778. (e) Mansuy, D.; Bartoli, J. F.; Momenteau, M. *Tetrahedron Lett.* **1982**, *23*, 2871. (f) Lindsay-Smith, Sleath, P. R. *J. Chem. Soc., Perkin Trans. 2* **1982**, 1009. (g) Groves, J. T.; Nemo, T. E. *J. Am. Chem. Soc.* **1983**, *105*, 5786. (h) Groves, J. T.; Myers, R. S. *Ibid.* **1983**, *105*, 5791. (i) Groves, J. T.; Nemo, T. E. *Ibid.* **1983**, *105*, 6243.

0002-7863/86/1508-3266$01.50/0